Optimization of Convex Shapes: An Approach to Crystal Shape Identification *

Timo Eirola Toni Lassila

January 20, 2010

Abstract

We consider a shape identification problem of growing crystals. The shape of the crystal is to be constructed from a single interferometer measurement. This is an ill-posed inverse problem. The forward problem of interferogram from shape is injective if we restrict the problem to convex shapes with known boundary. The problem is formulated as a shape optimization problem. Our aim is to solve this numerically using the gradient descent method. In the numerical computations of this paper we study the behavior of the approach in simplified cases. Using H^1-gradients (inner products) acts as a regularization method. Methods for enforcing the convexity of shapes are discussed.

1 Introduction

Shape optimization is a field of mathematical optimization concerned with finding the shape (bounded open set with Lipschitz boundary) that minimizes a given cost functional. Boundary variational techniques can be used to compute sensitivities of functionals with respect to shape. Comprehensive texts on the topic of shape analysis include [10] and [17].

We consider a shape identification problem of finding the shape of a growing ^{3}He crystal that best fits the interferogram produced in a Fabry-Pérot interferometer. Based on physical principles it is assumed that the crystal shape is *convex at all times*. For an overview of the growth process of ^{3}He crystals and the interferometer setup, see [19].

The restriction to convex shapes can be used as a simplification tool in shape optimization problems. In [6] the authors showed the existence of solutions to very generic shape optimization problems with the constraint that the shapes were convex. In our problem of determining shape from interferogram the operator solving the forward problem is generally not injective if the shapes are

* *Eirola T. and Lassila T.: Optimization of convex shapes: an approach to crystal shape identification. Proceedings of the 2nd International Conference on Scale Space Methods and Variational Methods in Computer Vision, Voss, Norway, June 2009, pp.660-671, 2009.* The original publication is available at `http://www.springerlink.com/content/x2091u5661757513/`. This work has been supported by the *Academy of Finland* (decision number 107290/04). We would like to thank Heikki Junes from the Low Temperature Laboratory at TKK for his input and introducing us to this problem.

allowed to be nonconvex. We prove that if the convexity assumption holds and the height of the shape at the boundary of the computational domain is known then the shape identification problem does have a unique solution.

It has been previously noted that the convexity constraint can be difficult to handle in numerical computations, especially in higher dimensions. It is known that pointwise conditions, such as curvature conditions, can fail to guarantee convexity for functions sampled at discrete points. For further discussion on this point, see [1].

Methods for optimization in the family of convex functions have been previously studied in [1, 7, 8, 9, 13]. In contrast to most of these approaches we do not write a strict convex constraint system, but instead use a penalization method that allows convexity to be temporarily broken when it is beneficial to the convergence of the iteration.

The shape identification problem is solved using level set methods and gradient descent for shapes. Methods for convexification by evolution equations, such as the level set method, have been previously considered in [12, 20]. As is typical for ill-posed inverse problems, the presence of experimental noise in the measurements requires some type of regularization. We demonstrate that using H^1-gradients (inner products) for the shape gradients acts as a form of regularization.

2 Shapes and Shape Evolution

2.1 Representing Shapes

We first define the notation. The computational domain $D \subset \mathbb{R}^d$, $d \in \{1, 2\}$, is a convex bounded open set. We consider convex *shapes* (open sets with Lipschitz boundary) $\Omega \subset D \times \mathbb{R}^+$, which are supported by D from below, that is to say

$$\langle \vec{n}(\vec{x}), \vec{e}_3 \rangle < 0 \quad \Longrightarrow \quad x_3 = 0 \ , \tag{1}$$

where $\vec{n}$ is the outward normal vector field on the surface $\partial\Omega$.

A convex shape Ω supported by D can be represented in many ways. One is to give a Lipschitz function $\phi : D \times \mathbb{R}^+ \to \mathbb{R}$ such that

$$\Omega = \{\vec{x} \ : \ \phi(\vec{x}) < 0\}, \quad \Omega^c = \{\vec{x} \ : \ \phi(\vec{x}) \geq 0\} \tag{2}$$

and $|\nabla\phi|$ nonvanishing on $\partial\Omega$. Then ϕ is called an implicit function or a level set function for Ω. An alternative representation of Ω is with a function $u : D \to \mathbb{R}^+$ defined as

$$u(x_1, x_2) = \sup \ \{x_3 \geq 0 \ : \ \phi(x_1, x_2, x_3) \leq 0\} \ , \tag{3}$$

where ϕ is an implicit function for Ω. We call this the height function of Ω. Note that if Ω is convex then u is concave. Denote by $\mathcal{C} \subset H^1(D) \cap C(\overline{D})$ the set of concave functions on D that are continuous on $\overline{D}$. We also define $\mathcal{C}_h \subset \mathcal{C}$ as the subset of concave functions that are equal to h on the boundary ∂D for a given function $h : \partial D \to$
$mathbbR^+$.

2.2 Level Set Methods

Consider an initial shape Ω_0 and an evolution its boundary $\partial\Omega_0$ under a smooth velocity field $\vec{v}(\vec{x},t)$. When the shape $\Omega(t)$ at time t is represented by an implicit function $\phi(\cdot,t)$, we have an Eulerian representation of the evolution of the implicit function in time

$$\phi_t(\vec{x},t) + v_n(\vec{x},t)|\nabla\phi(\vec{x},t)| = 0 \ , \tag{4}$$

where v_n is the component of $\vec{v}$ in the outward normal direction of $\partial\Omega$. This is called a level set equation. Level set methods are a generic framework of nonlinear hyperbolic-parabolic PDEs for implicit functions that can be used to model evolution of shapes under certain types of flows. For a generic introduction into level set methods, see [16]. For a survey of level set methods specifically in inverse problems, see [5].

3 Shape Optimization

3.1 Shape Derivatives

Let $J(\Omega) : \Sigma \to \mathbb{R}$ be a shape functional defined on some family of admissible shapes Σ. The derivative with respect to shape at Ω_0 in the direction of the smooth velocity field $\vec{v}$ is defined as the limit

$$dJ(\Omega_0;\vec{v}) = \lim_{t\to 0^+} \frac{J(\Omega_t) - J(\Omega_0)}{t} \tag{5}$$

when it exists. With some general assumptions (see Chap. 8 of [10] for details) this expression is bounded and linear with respect to $\vec{v}$, and has support only on the boundary of Ω_0:

$$dJ(\Omega_0;\vec{v}) = \int_{\partial\Omega_0} D \cdot v_n \, dS \ . \tag{6}$$

Using the shape derivative (6) the shape functional can be expanded as

$$J(\Omega_t) = J(\Omega_0) + t \cdot dJ(\Omega_0;\vec{v}) + o(t) \ . \tag{7}$$

For a given Hilbert space $H(\partial\Omega_0)$ we look for the unique function $\nabla_{\mathrm{S}} J \in H(\partial\Omega_0)$ such that

$$dJ(\Omega_0;\vec{v}) = \langle \nabla_{\mathrm{S}} J, v_n \rangle_H \ . \tag{8}$$

Then $\nabla_{\mathrm{S}} J$ is the shape gradient of J with respect to the chosen inner product. If the velocity normal field v_n is chosen to be the negative shape gradient $v_n = -\nabla_{\mathrm{S}} J(\Omega_0)$ we have

$$J(\Omega_t) = J(\Omega_0) - t \cdot ||dJ(\Omega_0)||^2_{H(\partial\Omega_0)} + o(t) < J(\Omega_0) \tag{9}$$

for sufficiently small $t > 0$. This is the method of gradient descent for shape optimization. The negative gradient flow can be efficiently implemented with numerical level set methods.

3.2 Convexity Constraints

To obtain level set methods that preserve the convexity of the shape we follow the basic idea of constrained gradient descent. Let $G(\Omega)$ be a shape constraint functional. We consider the constrained shape optimization problem

$$\min_{\Omega} \quad J(\Omega) \tag{10}$$

subject to $G(\Omega) = 0$. Then if J and G are shape differentiable and there exist shape gradients $\nabla_S J$ and $\nabla_S G$, we let μ be a Lagrange multiplier and obtain the necessary conditions for a constrained minimum

$$\nabla_S J(\Omega) + \mu \nabla_S G(\Omega) = 0 \ , \tag{11}$$

$$G(\Omega) = 0 \ . \tag{12}$$

A C^2 shape in the plane is convex if the curvature of its boundary is nonnegative. In three dimensions a sufficient condition for convexity is that both principal curvatures of the surface must be nonnegative.

Let Ω be a convex shape with the height function u. Then the minimum curvature k_1 of the surface is given by

$$k_1 = -\frac{u_{x_1x_1} + u_{x_2x_2} + \sqrt{(u_{x_1x_1} - u_{x_2x_2})^2 + (2u_{x_1x_2})^2}}{\sqrt{1 + u_{x_1}^2 + u_{x_2}^2}} \ . \tag{13}$$

This follows from taking the smaller eigenvalue of the matrix representation of the second fundamental form. We extend k_1 to all of $D \times \mathbb{R}^+$ by setting

$$k_1(x_1, x_2, x_3) = k_1(x_1, x_2, u(x_1, x_2)) \quad \text{for all } x_3 \geq 0 \ . \tag{14}$$

Let Ω be supported by D and define $\widetilde{k} := k_1 \sqrt{1 + |\nabla u|^2}$. We use the constraint functional

$$G(\Omega) = \int_{\partial\Omega} u(\vec{x}) \max\{0, -k_1(\vec{x})\} \ dS \ . \tag{15}$$

This functional vanishes if and only if k_1 is everywhere nonnegative. The scaling by u is shown to be useful by the following computation. We reformulate the functional in terms of a change of integrals from $\partial\Omega$ to D. Then:

$$\begin{aligned} G(\Omega) &= \int_{\partial\Omega} \max\left\{0, -\frac{u}{\sqrt{1 + |\nabla u|^2}} \widetilde{k}\right\} \ dS = \int_D \max\left\{0, -u\widetilde{k}\right\} \ dx_1 \, dx_2 \\ &= \int_D \int_0^{u(x_1,x_2)} \max\left\{0, -\widetilde{k}\right\} \ dx_3 \, dx_2 \, dx_1 = \int_\Omega \max\left\{0, -\widetilde{k}\right\} \ dx \ . \end{aligned}$$

According to Theorem 4.2 of Chap. 8 in [10] this functional has the L^2 shape gradient

$$\nabla_S \widetilde{G} = \max\left\{0, -\widetilde{k}\right\} \ . \tag{16}$$

We obtain the penalty function formulation for the level set equation (4) with a convexity constraint

$$\phi_t + \left(v_n - \mu \max\left\{0, -\widetilde{k}\right\}\right) |\nabla \phi| = 0 \ , \tag{17}$$

with a penalty term $\mu > 0$. This method is a version of the min/max curvature flows studied in [14], since

$$\phi_t + v_n|\nabla\phi| = \mu \min\{0, k_1\}|\nabla\phi| \ . \tag{18}$$

Furthermore, the minimum curvature flow will convexify the initial shape, justifying our choice of the constraint functional (15). The following theorem was proven in [20]:

Theorem 1. *In the case that $v_n \equiv 0$, the viscosity solution of the equation (17) converges towards the convex hull of the initial shape Ω_0 as $t \to \infty$.*

4 A Problem in ^{3}He Crystal Imaging

4.1 Fabry-Pérot Interferometer Measurement of a Crystal

The formation of faceted crystals in low-temperature ^{3}He has been the subject of study in the low temperature physics community. It is known that at below 200 mK temperatures smooth facets appear that correspond to orientations of the lattice planes. The problem of predicting which facets appear at which temperature is still open. It is known that as the temperature is increased past the so called roughening limit the facets become rounded out and no longer appear. The theoretical roughening limit is much higher than what has been observed in practical experiments.

We consider an experimental setup where liquid ^{3}He at temperature below 200 mK is placed between the two plates of a Fabry-Pérot interferometer. Overpressure is then exerted to allow the creation of crystals to occur. As light passes through the crystals, a diffraction pattern is observed on a CCD imaging array. By relating the intensity of the interferogram to the phase delay through the crystal at each point we can determine the shape of the crystal and the orientation of all the facets.

4.2 Convexity of Crystals and the Growth Process

The growth of crystals is governed by three principal forces: the external work done to the system by the driving overpressure, the surface tension between the liquid and solid Helium, and gravity. When the crystal growth process is sufficiently slow we can assume that at each measurement the crystal has achieved thermal equilibrium. The crystal shape is then determined by minimizing a surface energy. This leads to an anisotropic mean curvature flow that models the growth process of crystals [21]. It is known that such flows preserve convexity of the shapes [3]. We therefore assume that, apart from small irregularities, the thermal equilibrium shape is also convex. This assumption has been verified in experimental measurements.

4.3 Inverse Problem of Shape from Interferogram

Let $D = [0,1]^2$ be the domain of the interferogram and $f : D \to \mathbb{R}$ a function that gives the intensity of the interference pattern at each point on the CCD. The physical parameters are Δn_{sl}, the difference between the refractive indices

of the solid and liquid ^{3}He, and λ, the interferometer laser wavelength, and $a(\vec{x})$ the amplitude.

The intensity of the interference pattern at each point is given approximately by

$$\mathcal{F}(u)(\vec{x}) = a(\vec{x})\,\varphi(\frac{\Delta n_{\rm sl}}{\lambda}u(\vec{x})) = f(\vec{x}) \ , \tag{19}$$

where $\varphi : \mathbb{R} \to [-1, 1]$ is a continuously differentiable piecewise strictly monotone waveform function. Note that this definition forbids square or sawtooth type waveforms. To simplify things we assume the laser amplitude to be almost constant and known, $a(\vec{x}) \approx \widetilde{a}$. The inverse problem to be solved is: given an interferogram $f \in L^2(D)$ of measured intensities (with noise), deduce the shape of the crystal Ω.

This problem can be posed as a mathematical shape optimization problem. Let Ω be a convex trial shape supported by D. Denote the bottom part of the surface of the shape as $\Gamma_b := \partial\Omega \cap D$. We consider the shape functional with the L^2-norm

$$J(\Omega) = \tfrac{1}{2}\int_{\partial\Omega\setminus\Gamma_b} |\varphi(x_3) - \mathcal{S}f(x_1, x_2)|^2 \, dS \ , \tag{20}$$

where φ is a continuously differentiable and piecewise strictly monotone function and $\mathcal{S} : L^2(D) \to H^1(D)$ is a smoothing operator. The corresponding mathematical shape optimization problem is then

$$\min_{\Omega\in\Sigma^{\rm convex}_{\Gamma_b}} \quad J(\Omega) \ , \tag{21}$$

where $\Sigma^{\rm convex}_{\Gamma_b}$ is a family of convex shapes with Γ_b fixed. The choice of this family of will be discussed later. We have the following existence theorem from [6]:

Theorem 2. *Let f be such that $\mathcal{S}f$ is continuous. Then the shape optimization problem (21) has at least one solution.*

4.4 Is the Inverse Problem Uniquely Solvable?

It is possible to construct examples that show that in the absence of a convexity constraint the inverse problem of finding the shape Ω from its interference pattern f is not uniquely solvable even when we set a perimeter constraint such as requiring Γ_b to be fixed. But if we require convexity and fix u on the boundary $\partial\Gamma_b$, we have the following result:

Theorem 3. *Let $D \subset \mathbb{R}^d$ be a bounded convex open set and Γ its boundary. Fix a function $h \in C(\Gamma)$ on the boundary. Let $\mathcal{C}_h$ be the family of concave functions $u : \overline{D} \to \mathbb{R}$ in $C(\overline{D})$ such that $u|_\Gamma = h$. Let the operator $\mathcal{F} : H^1(D) \to H^1(D)$ be defined as*

$$(\mathcal{F}u)(\vec{x}) = \varphi(u(\vec{x})) \ . \tag{22}$$

where φ is a continuously differentiable and piecewise strictly monotone function. Then the restriction of $\mathcal{F}$ into $\mathcal{C}_h$ is injective.

Proof. Case $d = 1$:

Let $u, v : [a, b] \to \mathbb{R}$ be distinct concave functions such that $u(a) = v(a)$, $u(b) = v(b)$, and that $\varphi(u) \equiv \varphi(v)$. Let $(\xi, \eta) \subset [a, b]$ be any open interval where

$u \neq v$ but $u(\xi) = v(\xi)$ and $u(\eta) = v(\eta)$. Without loss of generality we assume $u > v$ on (ξ, η). Since φ is continuously differentiable and $\varphi(u(\xi)) = \varphi(v(\xi))$ from the inverse function theorem it follows that $\varphi'(u(\xi)) = 0$.

From the assumption that φ is piecewise strictly monotone follows that φ' has only isolated zeros. Thus the local behavior of φ near $u(\xi)$ can be of only two types, a) or b), as shown in Fig. 1.

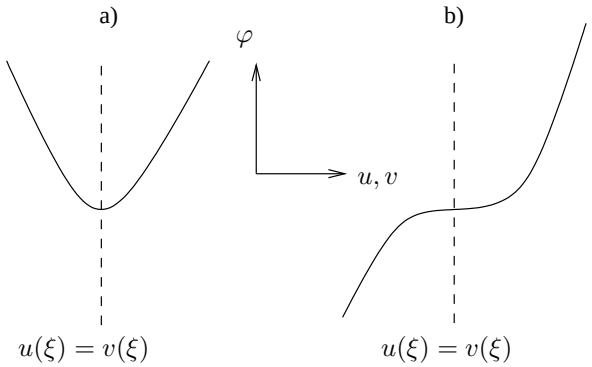

Figure 1: The different kinds of possible local behavior of the function $\varphi(u)$ near a bifurcation point ξ.

Since u is concave there exists an interval $(\xi, \xi+\varepsilon)$ where it is either constant, increasing, or decreasing:

1. If u was constant in some interval $(\xi, \xi + \varepsilon)$ then so would be $\varphi(v)$. But because φ' cannot vanish in any neighborhood of $u(\xi)$ this would mean that v would also be constant in $(\xi, \xi + \varepsilon)$, a contradiction. So neither u nor v can be locally constant past the bifurcation point ξ.

2. Assume that u is increasing in some interval $(\xi, \xi+\varepsilon)$ and the local behavior of φ is like in a). Then v must be decreasing in $(\xi, \xi + \varepsilon)$.

3. Assume that u is decreasing in some interval $(\xi, \xi + \varepsilon)$ and the local behavior of φ is like in b). But since $u > v$, case b) is impossible.

Thus immediately after the bifurcation point ξ we must have u increasing and v decreasing. Using the same argument at η we get that u must be decreasing and v increasing in some interval $(\eta - \varepsilon, \eta)$. But v is concave and cannot be first decreasing and later increasing, a contradiction.

Case $d \geq 2$:

For every pair of points $\vec{x}, \vec{y} \in \Gamma$ we take the line segment L connecting $\vec{x}$ to $\vec{y}$ and look at the restrictions $u|_L, v|_L$, which are concave functions of one variable. Since u, v coincide on all such segments L they are equal everywhere. □ □

We remark that in when the measurement is noisy we can lose the uniqueness of the solution. This is due to the fact that the range of the forward operator $\mathcal{F}$ is nonconvex, and thus if the measurement f lies outside the range of $\mathcal{F}$ the minimization problem (21) can have multiple solutions.

4.5 Formulation for the H^1-variation of a Shape Functional

To solve optimization problem (21) using the gradient descent method we must find the shape gradient of the functional given by (8). While the gradient could be computed only in the L^2 inner product, we prefer the H^1 inner product since the resulting gradients are smoother and hopefully also lead to a numerically more robust algorithm. The need for regularizing the shape variations is well-established in the literature, but the relation with regularization of ill-posed inverse problems perhaps less so. The effect of different inner products on the convergence of the gradient descent iteration was studied in more detail in [4].

Theorem 1. *Consider the shape functional for d-dimensional convex shapes* $\Omega \subset D \times \mathbb{R}^+$*:*

$$J(\Omega) = \int_{\partial\Omega \setminus \Gamma_b} g(\vec{x}, \vec{n})\, dS \ , \tag{23}$$

where $g(\vec{x}, \vec{n})$ *is* H^1 *with respect to both arguments. Then* J *is shape differentiable and the shape derivative* $dJ(\Omega; \vec{v})$ *with respect to a normal variation* $v_n \in H_0^1(D)$ *is given by*

$$dJ(\Omega; \vec{v}) = \int_D \big[-\nabla_n g \cdot \nabla v_n + (\nabla_x g \cdot \vec{n} + \kappa g) v_n \big] |F|\, d\xi \ , \tag{24}$$

for all $v_n \in H_0^1(D)$*, where* $|F| := \sqrt{1 + |\nabla u|^2}$ *is the change of integrals term given by* u *the height function of the convex shape.*

Proof. The details are given for example in [18]. Here we reproduce only the general procedure. Let Ω be given and ϕ its implicit function. Then according to the coarea formula [11] gives

$$J(\Omega) \quad = \quad \int_{\partial\Omega \setminus \Gamma_b} g(\vec{x}, \vec{n})\, dS = \int_{\mathbb{R}^d} g(\vec{x}, \frac{\nabla\phi}{|\nabla\phi|})\, |\nabla\phi|\, \delta(\phi)\, \chi_{\Gamma_b^c}\, d\vec{x} \ .$$

The variation can now be performed in terms of ϕ. Let $v_n = -\psi/|\nabla\phi|$ be an extension velocity field to the entire $\mathbb{R}^d$ such that $\psi|_{\Gamma_b} \equiv 0$, i.e. the base remains fixed. The Gâteaux derivative is, after some computations, given by

$$dJ(\Omega; \vec{v}) = \frac{d}{d\tau} J(\phi + \tau\psi) = \int_{\mathbb{R}^d} \left(-\frac{\psi}{|\nabla\phi|} \right) \nabla \cdot \left[\nabla_n g + g \frac{\nabla\phi}{|\nabla\phi|} \right] |\nabla\phi| \delta(\phi)\, dx \ .$$

Integration by parts gives

$$\int_{\partial\Omega} \nabla \cdot (\nabla_n g)\, v_n\, dS = -\int_{\partial\Omega} \nabla_n g \cdot \nabla v_n\, dS$$

and the result follows by using the coarea formula in the other direction and noting that $\vec{n} = \nabla\phi/|\nabla\phi|$ and $\kappa = \nabla \cdot \vec{n}$ is the mean curvature of $\partial\Omega$. □ □

We can thus compute the negative shape gradient of J with respect to the H^1 inner product as the solution $w \in H_0^1(D)$ of the elliptic equation

$$\int_D (\nabla v_n \cdot \nabla w + v_n w)\, d\xi + \int_D (\alpha v_n + \beta \cdot \nabla v_n)\, d\xi = 0, \quad \text{for all } v_n \in H_0^1(D) \ , \tag{25}$$

where $\alpha = |F|\,(\nabla_x g \cdot \vec{n} + \kappa g)$ and $\beta = -|F|\nabla_n g$ as in Lemma 1, plus homogeneous Dirichlet boundary conditions. For the convex constrained iteration it also beneficial to use the H^1-gradient of the constraint functional (15), which can be obtained by the same procedure from (16).

5 Numerical Experiments

5.1 Methodology

As a first approach to optimization of convex shapes we limit the numerical experiments to 1-d and choose $D = [0, 1]$. The questions to be answered are:

- Does the convexity constraint penalty term improve the quality of the recovered shapes?
- We would like to estimate the tensor of anisotropy of the mean curvature flow that drives the crystal formation process. Can reasonable estimates for the curvatures be obtained from the recovered shapes?

The quality of the recovered shapes was studied with two different crystal profiles (shown in Fig. 2). Case A represents a faceted crystal, while Case B is a smooth profile. For the forward model we used a sinusoidal waveform, $f(x) = \sin(\gamma u(x))$. To measure the error of the recovered shapes we generated a testing sample of 100 noisy realizations of the data f, each with 10% standard deviation, and took the mean L^2-error over this sample set.

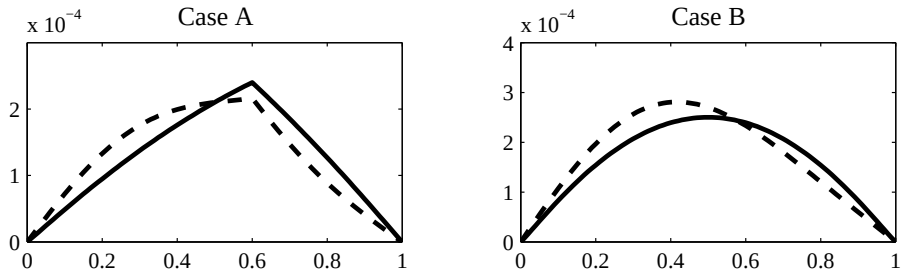

Figure 2: Left: True crystal shape (solid line) and initial guess (dashed line) for the test Case A. Right: Same for Case B.

At each descent step the shape derivative (24) was computed. The H^1-gradient was solved from equation (25). The normal velocity field was extended to the entire computational domain and the resulting level set evolution was solved using the Level set method toolbox [15] for Matlab. The gradient descent step size was chosen according to the Armijo rule [2] to obtain decreasing steps in the functional (20). The iteration was stopped when the recovered height function u changed less than 0.1% in the L^2-norm during the previous step. For the convex constrained iteration (17) we used a penalty parameter value of $\mu = 10^5$.

5.2 Choosing the Smoothing Operator $\mathcal{S}$

To construct the smoothing operator $\mathcal{S}$ in (20) we considered linear diffusion operators of the form

$$(\mathcal{S}f)(x_i) = (I - \delta D_{xx})^{-K} f(x_i), \quad K \in \mathbb{N} \ , \tag{26}$$

where D_{xx} is an operator giving the discrete approximation of the second derivative of f at x_i. The simplest choice is the symmetric difference approximation for the second derivative (in the 1-d case)

$$D_{xx} = \frac{f(x_{i+1}) - 2f(x_i) + f(x_{i-1})}{\Delta x^2} \ . \tag{27}$$

This difference approximation tends to smooth out especially the corners of f, so that for faceted profiles we should choose K moderately small. We chose $\delta = 0.01$ and considered the cases $K = 0$ (no smoothing) and $K = 100$ (with smoothing).

5.3 Comparison of Convergence with and without the Convexity Constraint

The first observation we made was that the L^2-gradient descent iteration in general *does not work at all*. The computed boundary variations were too oscillatory. After an H^1-gradient was implemented the regularization was enough to provide local convergence from an initial guess that had 15%-20% relative L^2-error.

In Table 1 we list the accuracy of the obtained shapes by the relative L^2-error from the true crystal shape. We note that in both cases the recovered solutions were roughly within 3% of relative error. This remained the case even with convexity constraints and smoothing of the data. The sharp corner of Case A also produced more error than the smooth profile of Case B.

Table 1: Relative L^2-error from the true profile u obtained by the unconstrained ($\mu = 0$) and convex constrained ($\mu = 10^5$) iterations with and without smoothing.

Case	No smoothing $\mu = 0$	No smoothing $\mu = 10^5$	With smoothing $\mu = 0$	With smoothing $\mu = 10^5$
A	1.71 %	2.61 %	1.98 %	2.63 %
B	0.47 %	0.51 %	0.47 %	0.61 %

5.4 Estimating the Curvature(s) of the Crystal Surface

One way of evaluating the quality of the recovered crystal shapes is to see if useful estimates for the curvature(s) of the crystal surface can be obtained. We ran both the unconstrained and convex constrained iterations for Case A. We also tested the effect of increasing K in the smoothing operator (26).

The obtained curvatures are plotted in Fig. 3. In this case the curvature should be zero almost everywhere with a singularity at one point. None of the

curvature estimates are free from numerical artifacts. The convex constrained solution gives curvatures that are nearly nonnegative everywhere. The effect of added smoothing is to dampen the oscillations of the recovered curvatures.

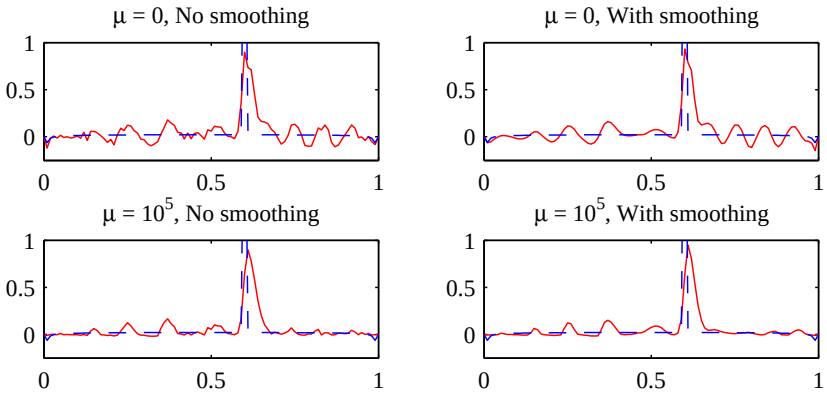

Figure 3: Estimated curvatures for the Case A obtained with the unconstrained and convex constrained iterations, with and without smoothing of the data. The true curvature is denoted by a dashed line.

6 Conclusions

The inverse problem of crystal shape identification from a single interferogram is uniquely solvable if the shape is required to be convex and we have boundary data available. Numerical level set methods can be used to solve such problems with the gradient descent method. We added a penalty term to enforce convexity of the shapes. By choosing H^1 shape gradients we introduced regularization to the problem. This allowed recovery of solutions of the otherwise ill-posed problem. We demonstrated that local convergence is obtained even when relatively large amounts of noise are present in the interferogram. The convex penalty term improved the quality of the recovered surface curvatures.

References

[1] N.E. Aguilera and P. Morin. Approximating optimization problems over convex functions. *Numer. Math.*, 111(1):1–34, 2008.

[2] L. Armijo. Minimization of functions having Lipschitz continuous first partial derivatives. *Pacific J. Math.*, 16(1), 1966.

[3] G. Bellettini, V. Caselles, A. Chambolle, and M. Novaga. Crystalline mean curvature flow of convex sets. *Arch. Ration. Mech. Anal.*, 179:109–152, 2005.

[4] M. Burger. A framework for the construction of level set methods for shape optimization and reconstruction. *Interfaces Free Bound.*, 5:301–329, 2003.

[5] M. Burger and S.J. Osher. A survey on level set methods for inverse problems and optimal design. *European Journal of Applied Mathematics*, 16(2):263–301, 2005.

[6] G. Buttazzo and P. Guasoni. Shape optimization problems over classes of convex domains. *J. Convex Anal.*, 4(2):343–351, 1997.

[7] G. Carlier and T. Lachand-Robert. Convex bodies of optimal shape. *J. Convex Anal.*, 10:265–273, 2003.

[8] G. Carlier, T. Lachand-Robert, and B. Maury. A numerical approach to variational problems subject to convexity constraint. *Numer. Math.*, 88:299–318, 2001.

[9] G. Carlier, T. Lachand-Robert, and B. Maury. H^1-projection into set of convex functions: A saddle point formulation. In *ESAIM: Proc. Vol.10*, pages 277–290, 2001.

[10] M.C. Delfour and J.-P. Zolésio. *Shapes and geometries - analysis, differential calculus, and optimization*. SIAM, 2001.

[11] H. Federer. *Geometric measure theory*. Springer-Verlag New York, 1969.

[12] W. Hinterberger and O. Scherzer. Variational methods on the space of functions of bounded Hessian for convexification and denoising. *Comput.*, 76:109–133, 2006.

[13] T. Lachand-Robert and É. Oudet. Minimizing within convex bodies using a convex hull method. *SIAM J. Optim.*, 16(2):368–379, 2005.

[14] R. Malladi and J.A. Sethian. Image processing: flows under min/max curvature and mean curvature. *Graph. Models Image Process.*, 58(2):127–141, 1996.

[15] I.M. Mitchell. The flexible, extensible and efficient toolbox of level set methods. *J. Sci. Comput.*, 2007. Online First.

[16] S.J. Osher and R. Fedkiw. *Level set methods and dynamic implicit surfaces*, volume 153 of *Applied Mathematics Sciences*. Springer-Verlag, 2002.

[17] J. Sokolowski and J.-P. Zolésio. *Introduction to shape optimization: shape sensitivity analysis*. Springer, 2003.

[18] J.E. Solem. *Variational problems and level set methods in computer vision - theory and applications*. PhD thesis, Lund University, 2006.

[19] V. Tsepelin, H. Alles, A. Babkin, R. Jochemsen, A.Ya. Parshin, I.A. Todoshchenko, and G. Tvalashvili. Morphology and growth kinetics of 3He crystals below 1 mK. *J. Low Temp. Phys.*, 129(5-6):489–530, 2002.

[20] L. Vese. A method to convexify functions via curve evolution. *Commun. Partial Differential Equations*, 24(9):1573–1591, 1999.

[21] J.S. Wettlaufer, M. Jackson, and M. Elbaum. A geometric model for anisotropic crystal growth. *J. Phys. A*, 27:5957–5967, 1994.